Time-domain structural vibration simulations by solving the linear elasticity equations with the discontinuous Galerkin method

TIME-DOMAIN STRUCTURAL VIBRATION SIMULATIONS BY SOLVING THE LINEAR ELASTICITY EQUATIONS WITH THE DISCONTINUOUS GALERKIN METHOD

Indra Sihar and Maarten Hornikx

Eindhoven University of Technology, Department of Built Environment, Eindhoven, the Netherlands
email: i.sihar@tue.nl

Pranowo

Universitas Atma Jaya Yogyakarta, Teknik Informatika Study Program, Yogyakarta, Indonesia

In the field of building acoustics, an efficient solution of the linear elasticity equations for vibro-acoustic problems is of interest. The focus of this work is on the structural part, with plate vibration problems in particular. The linear elasticity equations in the stress-velocity formulation are solved in the time-domain for the three-dimensional plate problem. The numerical solution is obtained through the Runge-Kutta discontinuous Galerkin method, which has the potential to be highly parallelizable and thereby computationally very efficient. Numerical aspects of applying the discontinuous Galerkin method to this problem are discussed, especially on the force excitation and the boundary conditions of the plate problem. The accuracy of applying the discontinuous Galerkin solution is presented by comparing its results to results from analytical solutions. Several scenarios of plate variations with different boundary conditions are simulated to demonstrate the capabilities of the method.
Keywords: plate vibration, discontinuous Galerkin method, low frequencies, time domain

1. Introduction

To design a proper sound insulation, prediction of sound transmission through building components is needed. Sound transmission through a panel is frequently predicted using two analytical approaches. The first approach calculates sound transmission by simplifying the dynamics of the fluid or the structure. Often, this approach idealises the impinging sound wave to the structure as a plane wave or assuming a diffuse field condition. The calculation models of this approach include plane wave transmission through an infinite plate, and transmission of a diffuse sound field through a baffled plate [1]. Moreover, at high frequencies, when the structural field is also a diffuse field, the statistical energy analysis (SEA) could be utilized to calculate sound transmission. This approach is used extensively in many engineering practice since it has a low computational cost. However, when the coupling between structure and fluid is strong, for instance at low frequencies, the first approach is not appropriate. This leads to the second approach where the dynamics of the fluid in a cavity is calculated and coupled with the dynamics of the structure. One way to apply the second approach is by representing the unknown variables in each subsystem using a modal expansion method [1] [2]. Afterwards, continuity conditions in the fluid-structure interface are satisfied. In case of light fluid loading, structural mode shapes can be obtained *in-vacuo*, and room mode shapes can be obtained by assuming the structure is rigid.

The more general way to conduct the second approach is by numerically solving the structure and fluid problem using the same variables for both media, i.e. the displacement/velocity and stress terms [3]. This methodology can be applied, for instance, using linear elasticity equations. There are some advantages of using the linear elasticity equations to solve the sound transmission problem. For example: a separate model between thin or thick structure is not needed, and changes in cross section area due to stiffeners, junctions, or any discontinuities could be treated directly in the model. In this paper, as a first step to solve the fluid-structure interaction problem to model sound insulation of a complex building structure, the dynamics of a plate as a three-dimensional structure are modelled by solving the linear elasticity equations using a numerical method.

The linear elasticity equations have been used frequently to model seismic wave problems, examples of numerical solutions in the time domain can be found in the work of Vireux using the finite difference method [4], and in the work of Dumbser using an arbitrary high-order derivatives discontinuous Galerkin (DG) method [5]. In the field of building acoustics, the linear elasticity equations have been used to model a floor system, and a numerical solution has been developed by Toyoda using the finite difference method [6]. In this paper, using the same equations for the plate vibration problem, the nodal DG method is used to get the solution. This method is in particular of interest as it is very favourable to carry out DG calculations by a parallel implementation, opening opportunities of solve real-world problems in a reasonable computation time. Furthermore, hybrid approach on nodal DG with Fourier Pseudospectral time-domain has been conducted by Pagán Muñoz to solve the acoustic propagation problem in fluid [7], which has the possibility to be coupled with the current structural vibration problem. The nodal DG is one method of applying the DG method; it is developed by Hesthaven and Warburton [8] and has been used widely to solve electromagnetic and fluid mechanics problems. In the next section, brief descriptions of the method including source term and boundary conditions are described. Finally, the plate mobility solution for different sets of boundary conditions are presented and compared with the thin plate solution.

2.   Formulation

2.1   Linear Elasticity Equations

In solid isotropic media, linear vibrations can be modelled by equations of motion and constitutive equations; this set of equations is known as the linear elasticity equations. By having the time derivative of the stress-strain constitutive equations, the isotropic linear elasticity equations can be written in the stress-velocity form using three-dimensional Cartesian coordinates as:

$$\frac{\partial \mathbf{q}}{\partial t} + \nabla \cdot (\mathbf{A}\mathbf{q}) = \mathbf{g} , \qquad (1)$$

$$\mathbf{A} = \mathbf{A}_x n_x + \mathbf{A}_y n_y + \mathbf{A}_z n_z ,$$

$$\mathbf{A} = \begin{bmatrix}
0 & 0 & 0 & -n_x/\rho & 0 & 0 & -n_z/\rho & 0 & -n_y/\rho \\
0 & 0 & 0 & 0 & -n_y/\rho & 0 & 0 & -n_z/\rho & -n_x/\rho \\
0 & 0 & 0 & 0 & 0 & -n_z/\rho & -n_x/\rho & -n_y/\rho & 0 \\
-(\lambda+2\mu)n_x & -\lambda n_y & -\lambda n_z & 0 & 0 & 0 & 0 & 0 & 0 \\
-\lambda n_x & -(\lambda+2\mu)n_y & -\lambda n_z & 0 & 0 & 0 & 0 & 0 & 0 \\
-\lambda n_x & -\lambda n_y & -(\lambda+2\mu)n_z & 0 & 0 & 0 & 0 & 0 & 0 \\
-\mu n_z & 0 & -\mu n_x & 0 & 0 & 0 & 0 & 0 & 0 \\
0 & -\mu n_z & -\mu n_y & 0 & 0 & 0 & 0 & 0 & 0 \\
-\mu n_y & -\mu n_x & 0 & 0 & 0 & 0 & 0 & 0 & 0
\end{bmatrix} ,$$

$$\mathbf{q} = \begin{bmatrix} v_x & v_y & v_z & \tau_{xx} & \tau_{yy} & \tau_{zz} & \tau_{xz} & \tau_{yz} & \tau_{xy} \end{bmatrix}^T ,$$

$$\mathbf{g} = \begin{bmatrix} g_x & g_y & g_z & 0 & 0 & 0 & 0 & 0 & 0 \end{bmatrix}^T,$$

with $\mathbf{q}$ the vibration variables vector, v_i the velocity vector, τ_{ij} the stress tensor, and $\mathbf{g}$ the body force vector. $\mathbf{A}$ is the fluxes Jacobian which includes the material property: the density ρ, and the Lamé parameters λ, μ. The coefficients n_x, n_y, n_z are the unit normal of the control surface. The problem specification is completed by defining the problem domain, initial and boundary conditions. This set of equations consists of nine variables, and all derivative operators are of first order. In this study, the solution of the linear elasticity equations is obtained by evaluating the spatial differential operator using the nodal DG method, and integrating the time differential operator using the Runge-Kutta method.

2.2 Nodal Discontinuous Galerkin Method

To solve partial differential equations, the DG method discretizes the problem domain into several discontinuous conforming elements. On each element D, the problem's variational form is satisfied to obtain a solution where the unknown variables are approximated using a combination of basis functions. Moreover, the DG method solves the integration of numerical fluxes along the boundaries ∂D using a Riemann solver. In this study, the nodal approach of the DG method as presented by Hesthaven and Warburton is applied [8]. This approach uses the strong variational form and Lagrange interpolating polynomials $\varphi_p(\mathbf{x})$ as the basis function. For the local solution, unknown variables are expressed using summation of the basis function as:

$$\mathbf{q}_h(\mathbf{x},t) = \sum_{p=1}^{N_p} \mathbf{q}_h(\mathbf{x}_p,t)\varphi_p(\mathbf{x}), \tag{2}$$

where $\mathbf{q}_h$ is the local solution of Eqs. (1) for unknown variables $\mathbf{q}$, subscript p is the index of the basis function, and N_p is the maximum order of the basis function that is used. Using the interpolating polynomials as basis function, nodal DG distributes N_p number of nodes in each element. The details on the nodal distribution can be seen in the work of Hesthaven [8]. To obtain the strong form, Eqs. (1) are multiplied with a test function, where in Galerkin method the test function is same as the basis function. Afterward, integration over the volume V of each element is applied twice over the element:

$$\int_D \left[\frac{\partial \mathbf{q}_h}{\partial t} + \nabla.(\mathbf{A}\mathbf{q}_h) \right] \varphi_p dV = \int_D \mathbf{g}_h \varphi_p dV - \int_{\partial D} \mathbf{n}. \left[\mathbf{f}^* - \mathbf{A}\mathbf{q}_h \right] \varphi_p dS, \tag{3}$$

where $\mathbf{f}^*$ is the numerical flux, and $\mathbf{n}$ is the normal vector to the element boundary ∂D. In this study, to solve the Riemann problem a numerical flux from Godunov's method is used. The derivation of this flux can be seen in [5] [9], and reads as:

$$\mathbf{f}^* = \mathbf{R}\mathbf{\Lambda}^+\mathbf{R}^{-1}\mathbf{q}^- + \mathbf{R}\mathbf{\Lambda}^-\mathbf{R}^{-1}\mathbf{q}^+, \tag{4}$$

where $\mathbf{R}$ are the right eigen-vectors of matrix $\mathbf{A}$, $\mathbf{\Lambda}^+$ are the positive eigenvalues of $\mathbf{R}$, $\mathbf{\Lambda}^-$ are the negative eigen-values of $\mathbf{R}$, $\mathbf{q}^-$ are the element vibration variables on the element boundary, and $\mathbf{q}^+$ are the neighbour elements vibration variables that coincide with $\mathbf{q}^-$. By inserting Eq. (2) to Eq. (3), and exploring the orthonormal properties of the basis function, the final semi-discrete form of Eqs. (1) can be written as:

$$\mathbf{M}^D \frac{\partial \mathbf{q}_h}{\partial t} + \sum_{j=x,y,z} \mathbf{K}_j \mathbf{A}_j \mathbf{q}_h = \mathbf{M}^D \mathbf{g}_h - \sum_{i=1}^{b} \mathbf{M}^{\partial D_i} \left(\mathbf{f}^* - \mathbf{A}\mathbf{q}_h \right), \tag{5}$$

where $\mathbf{M}^D$ is the mass matrix of the element, $\mathbf{K}_j$ is the stiffness matrix on each spatial derivative, $\mathbf{M}^{\partial D_i}$ is the mass matrix of the element face i, and b is the number of faces on each element. These matrices are obtained by transforming all elements into a reference element, and pre-calculated for each element before time integration is conducted. Having this form, time integration is applied to march forward from the initial conditions. In this work, the low storage Runge-Kutta method of order 4 and with 5 stages is used. More details on the nodal DG method can be found in [8].

3. Plate vibration application

3.1 Problem setting

In this section, the plate vibration problem is described. There are three plates with a different thickness $h = 0.12\text{m}; 0.08 \text{ m}$; and 0.04 m. Each plate is made of concrete with Young's modulus 33.7 GPa, density 2300 kg/m^3, Poisson's ratio 0.225, and area $1.8 \times 1.2 \text{ m}^2$. The plate is illustrated in Fig. 1 using a Cartesian coordinate system with the origin at (0,0,0). The objective of the problem is to get the transfer mobility between force located at (0.42, 0.99, h) m (marked as a blue dot) and velocity located at (1.35, 0.99, h) m (marked as a red dot).
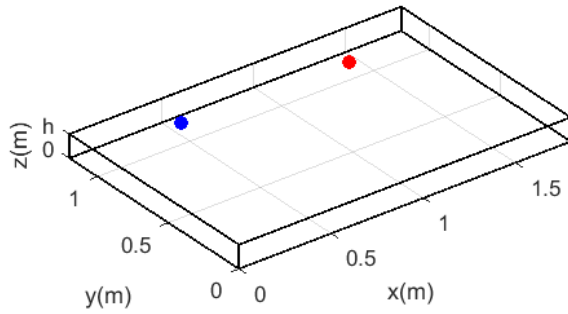

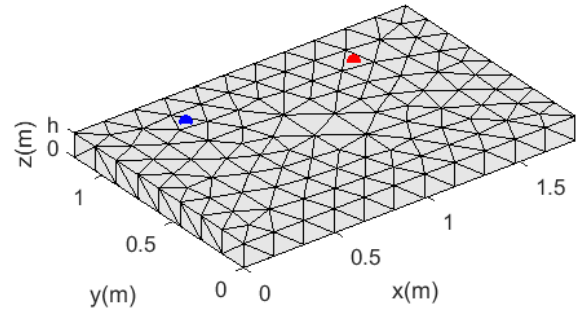Figure 1: Illustration of plate, and source and receiver position

Figure 2: Illustration of the used discretization.

The force function is a Ricker wavelet as defined in Eq. (6) with centre frequency $f_c = 500 \text{ Hz}$. This frequency is taken, since the interest frequency range is below 1kHz. In the simulation, a time delay $t_d = 5 \text{ ms}$ is given to get a smooth force function.

$$\tau_{zz}\left(\mathbf{x_0}, t\right) = \left(0.5 - \left(\pi f_c \left(t - t_d\right)\right)^2\right) \exp\left(\left(\pi f_c \left(t - t_d\right)\right)^2\right). \tag{6}$$

Table 1: Specification of boundary conditions in each case

Face	Free conditions	Clamped conditions	Simply supported conditions
$\partial\Omega_{top}$	$\tau_{iz} = 0$	$\tau_{iz} = 0$	$\tau_{iz} = 0$
$\partial\Omega_{bot}$	$\tau_{iz} = 0$	$\tau_{iz} = 0$	$\tau_{iz} = 0$
$\partial\Omega_{edge1}$	$\tau_{ix} = 0$	$v_i = 0$	$v_y = 0; v_z = 0; \tau_{xx} = 0;$ $\tau_{yy} = 0; \tau_{zz} = 0; \tau_{yz} = 0.$
$\partial\Omega_{edge2}$	$\tau_{iy} = 0$	$v_i = 0$	$v_x = 0; v_z = 0; \tau_{yy} = 0;$ $\tau_{xz} = 0; \tau_{xx} = 0; \tau_{xz} = 0.$

To complete the problem definition, boundary conditions should be ascribed to each plate face. The plate boundary conditions are given in three sets of cases: free conditions, clamped conditions, and simply supported conditions. The description of each condition case is given in Table 1. Where $\partial\Omega_{top}$ is the plate top face at $z = h$, $\partial\Omega_{bot}$ is the plate bottom face at $z = 0$, $\partial\Omega_{edge1}$ are the plate edge faces at $x = 0$ and $x = 1.8$, and $\partial\Omega_{edge2}$ are the plate edge faces at $y = 0$ and $y = 1.2$ with index i equal to x, y or z. To summarize, there are nine plate examples varying with thickness and boundary conditions. The details considering the simply supported conditions on a three-dimensional plate can be seen in the work of Srivinas [9].

3.2 Numerical setting

The plate is discretized using unstructured tetrahedral elements that are generated by the Gambit mesh generator. The maximum element size is 0.16 m for every plate case, and a mesh illustration can be seen in Fig. 2. In every numerical calculation, basis functions with maximum order three are used. By this setting, 20 nodes are created in each element. In the nodal DG, to update the solution on each element, the neighbour element information q^+ is needed. For nodes on the boundary faces, the value of q^+ is obtained from q^- and the condition at the surface, either a boundary condition from Table 2 or the source function. The methodology in defining q^+ is quite similar to the finite volume methodology while defining the ghost nodes. In Table 2, the counterpart of Table 1 as the numerical boundary condition settings is presented. In this table, the q^+ on each set of faces and case are given, with each index i, j equal to x, y or z.

Table 2: Boundary conditions settings in the nodal DG

Face	Free conditions	Clamped conditions	Simply supported conditions
$\partial\Omega_{top}$	$\tau_{iz}^+ = -\tau_{iz}^-$; $v_i^+ = v_i^-$	$\tau_{iz}^+ = -\tau_{iz}^-$; $v_i^+ = v_i^-$	$\tau_{iz}^+ = -\tau_{iz}^-$; $v_i^+ = v_i^-$
$\partial\Omega_{bot}$	$\tau_{iz}^+ = -\tau_{iz}^-$; $v_i^+ = v_i^-$	$\tau_{iz}^+ = -\tau_{iz}^-$; $v_i^+ = v_i^-$	$\tau_{iz}^+ = -\tau_{iz}^-$; $v_i^+ = v_i^-$
$\partial\Omega_{edge1}$	$v_i^+ = v_i^-$; $\tau_{ix}^+ = -\tau_{ix}^-$; $\tau_{yy}^+ = \tau_{yy}^-$; $\tau_{yz}^+ = \tau_{yz}^-$; $\tau_{zz}^+ = \tau_{zz}^-$.	$\tau_{ij}^+ = \tau_{ij}^-$; $v_i^+ = -v_i^-$	$v_y^+ = -v_y^-$; $v_z^+ = -v_z^-$; $\tau_{ii}^+ = -\tau_{ii}^-$; $\tau_{yz}^+ = -\tau_{yz}^-$; $\tau_{xz}^+ = \tau_{xz}^-$; $\tau_{xy}^+ = \tau_{xy}^-$; $v_x^+ = v_x^-$.
$\partial\Omega_{edge2}$	$v_i^+ = v_i^-$; $\tau_{iy}^+ = -\tau_{iy}^-$; $\tau_{xx}^+ = \tau_{xx}^-$; $\tau_{xz}^+ = \tau_{xz}^-$; $\tau_{zz}^+ = \tau_{zz}^-$.	$\tau_{ij}^+ = \tau_{ij}^-$; $v_i^+ = -v_i^-$	$v_x^+ = -v_x^-$; $v_z^+ = -v_z^-$; $\tau_{ii}^+ = -\tau_{ii}^-$; $\tau_{xz}^+ = -\tau_{xz}^-$; $v_y^+ = v_y^-$; $\tau_{yz}^+ = \tau_{yz}^-$; $\tau_{xy}^+ = \tau_{xy}^-$.

To insert the force, since it is acting on the boundary of the plate, the normal stress component $\tau_{zz}(\mathbf{x}_s, t)$ is defined on the face of the element where the force is located. First, the mesh face where the impact point is located should be identified. Then, following the LeVeque's work in finite volume method [10], the stress component of nodes at the face $\mathbf{x}_s$ is expressed using $\tau_{zz}^+(\mathbf{x}_s, t) = 2g_z(t)/A_0 - \tau_{zz}^-(\mathbf{x}_s, t)$, with face area A_s and g_z the body force in N. Other stress components are not specified, which lead to the following expressions: $\tau_{xx}^+(\mathbf{x}_s, t) = \tau_{xx}^-(\mathbf{x}_s, t)$, $\tau_{yy}^+(\mathbf{x}_s, t) = \tau_{yy}^-(\mathbf{x}_s, t)$, $\tau_{xz}^+(\mathbf{x}_s, t) = \tau_{xz}^-(\mathbf{x}_s, t)$, $\tau_{yz}^+(\mathbf{x}_s, t) = \tau_{yz}^-(\mathbf{x}_s, t)$, and $\tau_{xy}^+(\mathbf{x}_s, t) = \tau_{xy}^-(\mathbf{x}_s, t)$. It should be noted here that the force is acting on a finite area and not a point, since for a point the normal stress cannot be defined. Another approach is to apply a varying stress distribution on the area with maximum stress in a point of force insertion, but to fulfil the current objective and frequency range, the constant distribution is sufficient.

3.3   Thin plate reference

To validate the nodal DG method, the transfer mobilities of the plate examples are calculated using the thin plate theory, and the results are taken for comparison. The thin plate theory calculates the bending wave response of a plate due to a transverse point force using a modal expansion approach. This modal function should satisfy the given boundary conditions. The plate mobility by thin plate theory is given by:

$$\frac{v_z\left(x_r, y_r\right)}{F_z\left(x_s, y_s\right)} = i\omega \sum_{m=1}^{\infty} \sum_{n=1}^{\infty} \frac{\Phi_{m,n}\left(x_r, y_r\right) \Phi_{m,n}\left(x_s, y_s\right)}{\Lambda_{m,n}\left[\omega_{m,n}^2 - \omega^2\right]}, \tag{6}$$

with $\Phi_{m,n}$ the mode function of the plate, Λ_{mn} the norm of the plate, $\omega_{m,n}$ the natural angular frequency, ω the force angular frequency, x_r, y_r the location of the receiver point, and x_s, y_s the location of the source point. The indices m, n represent the numbers of the eigenmodes $\Phi_{m,n}$ in the x, y. In this work, the details of the modal functions for the given set of boundary conditions, and the natural angular frequencies, are adopted the work by Gardonio and Elliot [11].
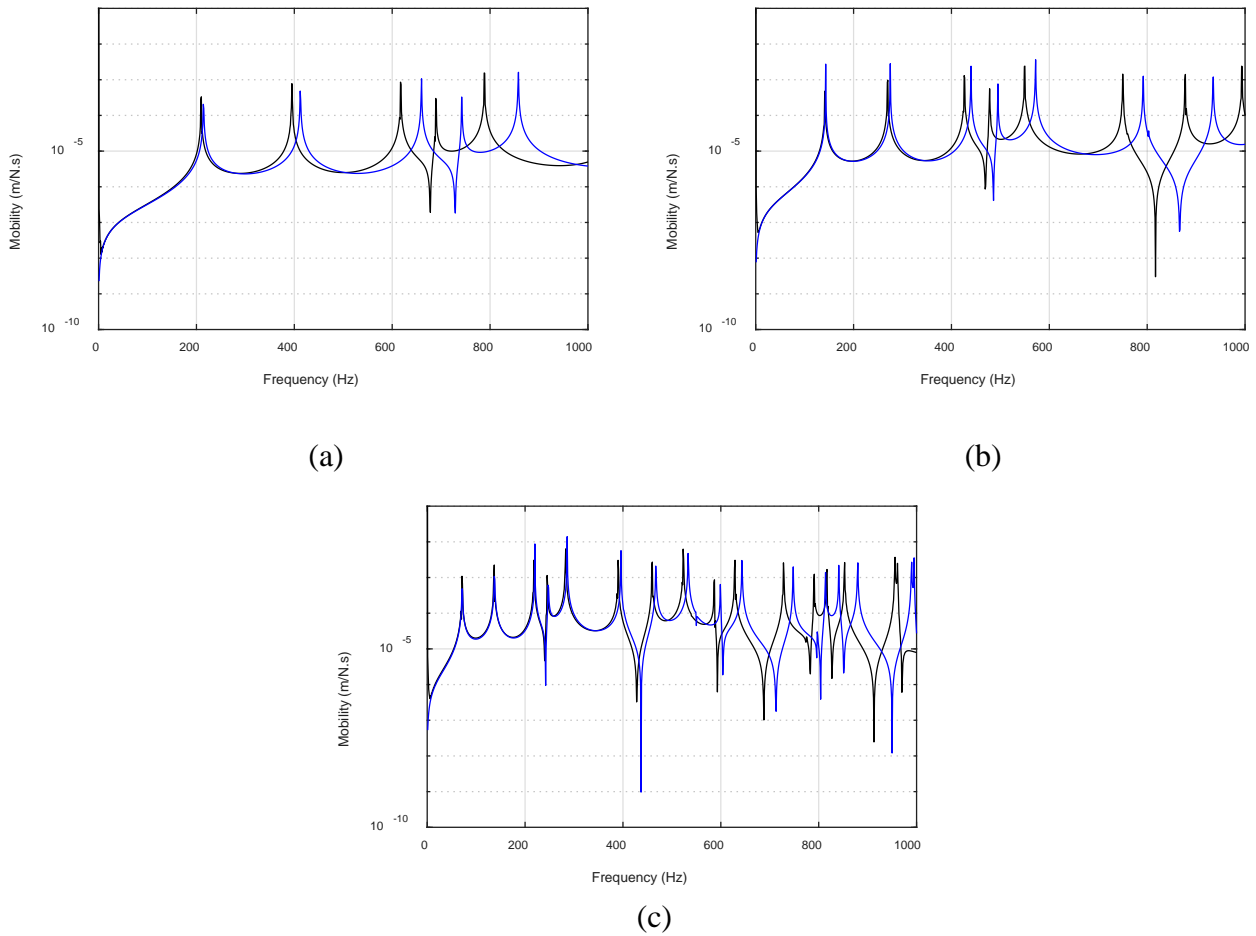
4.   Results and discussion
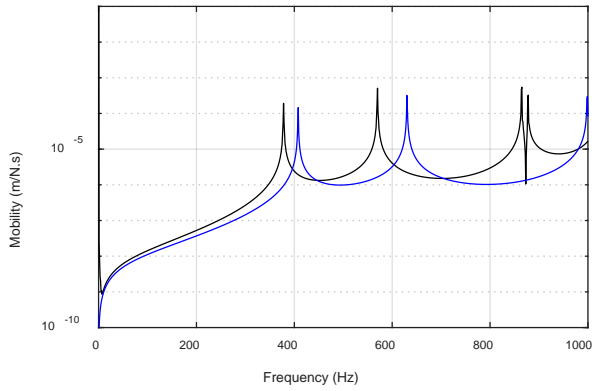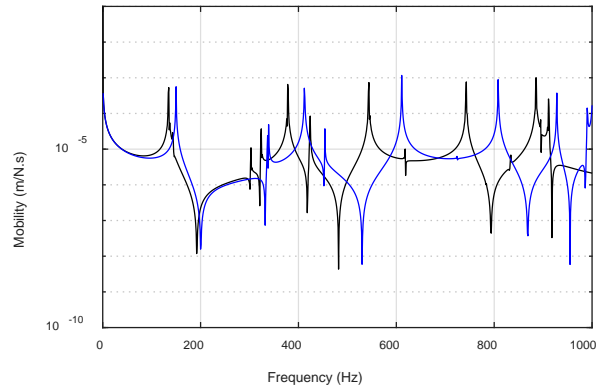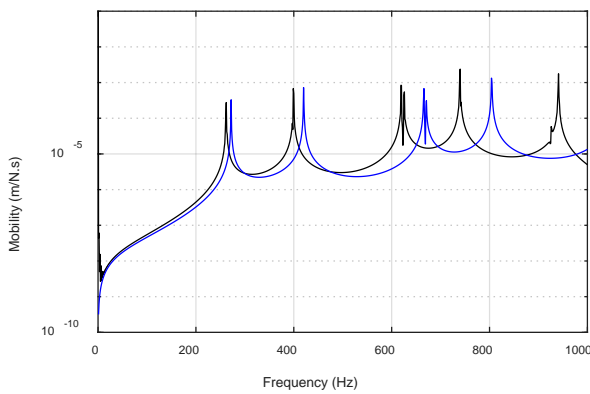

(a)

(b)

(c)

Figure 3: Plate mobility with simply supported boundary conditions for h = (a) 0.12m, (b) 0.08m, (c) 0.04m. Black line: nodal DG calculation, blue line: thin plate calculation.
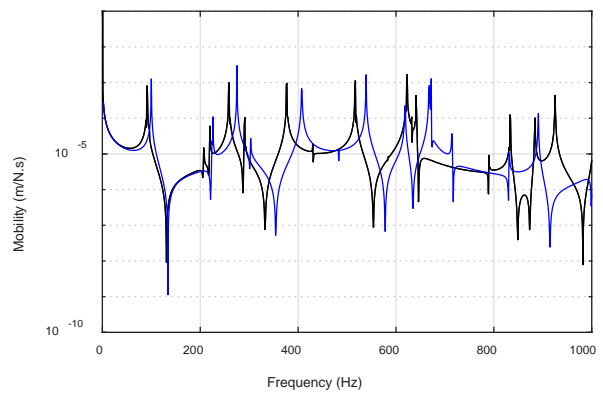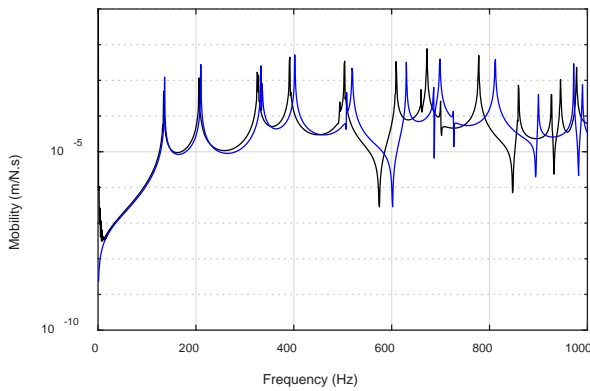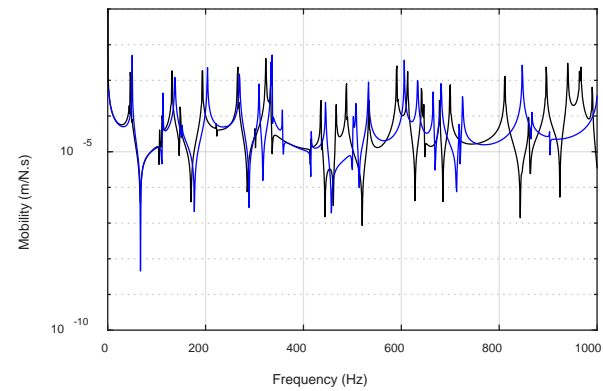
(a)

(b)

(c)

Figure 4: Plate mobility with clamped boundary conditions, for h = (a) 0.12m, (b) 0.08m, (c) 0.04m. Black line: nodal DG calculation, blue line: thin plate calculation.

Figure 5: Plate mobility with free boundary conditions, for h = (a) 0.12m, (b) 0.08m, (c) 0.04m. Black line: nodal DG calculation, blue line: thin plate calculation.

The nodal DG results shown in this section are obtained by having Fourier transformation of 1 s time domain numerical calculations. From Fig. 3 and Fig. 4, it can be seen that the DG results are in good agreement with the thin plate reference in the low frequencies region and for thinner plate. However, it can be seen that the discrepancy between results is increasing, as the frequency is getting higher. This discrepancy is expected, since the thin plate theory underestimates the plate inertia

and flexibility, which resulted in an overestimation of natural frequencies [12]. Results for the plate with free boundary conditions is shown are Fig. 5, showing a larger discrepancy than in figures 3 and 4. These discrepancies happen since the linear elasticity equations allow a variation of the displacement over the z-direction, which induces more modes. It should be noted that damping is not introduced into the DG model and in the thin plate reference. This creates sharp resonance peaks in the results.

5. Conclusions

To model vibrations in plates, a nodal time-domain discontinuous Galerkin method is presented to solve the linear elasticity equations. The free, clamped, and simply supported boundary conditions have been implemented in DG methodology, along with an external force insertion applied as a normal stress on the boundary. For all plate cases, the results show a reasonable agreement with the thin plate theory especially at low frequencies and at smaller thickness. To get a more accurate validation, the nodal DG solution should be compared to a thick plate theory. Further work will contain an extension to the fluid media such that fluid-structure problems in acoustics can be solved. In addition, an acceleration of the DG method by a parallel implementation will make this method highly useful for industrial applications.

Acknowledgements

REFERENCES

1 Osipov, A., Mees, P. and Vermeir, G. Low-Frequency Airborne Sound Transmission through Single Partitions in Buildings, *Applied Acoustics*, **52** (3), 273-288, (1997).

2 Neves e Sousa, A. and Gibbs, B. M., Low Frequency Impact Sound Transmission in Dwellings through Homogeneous Concrete Floors and Floating Floors, *Applied Acoustics*, **72** (4), 177-189, (2011).

3 Gladwell, G. M. L. and Zimmermann, G. On Energy and Complementary Energy Formulations of Acoustics and Structural Vibration Problems, *Journal of Sound and Vibration*, **3** (3), 233-241, (1966).

4 Virieux, J. P-SV Wave Propagation in Heterogeneous Media: Velocity-Stress Finite-Difference Method, *Geophysics*, **51** (4), 889-901, (1986).

5 Dumbser, M. and Käser, M. An Arbitrary High-Order Discontinuous Galerkin Method for Elastic Waves on Unstructured Meshes - II. The Three-Dimensional Isotropic Case, *Geophysical Journal International*, **167** (1), 319-336, (2006).

6 Toyoda, M. and Takahashi, D. Prediction for Architectural Structure-Borne Sound by the Finite-Difference Time-Domain Method, *Acoustical Science and Technology*, **30** (4), 265–276, (2009).

7 Pagán Muñoz, R. and Hornikx, M.C.J. A hybrid PSTD/DG method to solve the linearized euler equations: optimization and accuracy. *Proceedings of the 22nd AIAA/CEAS Aeroacoustics Conference*, Lyon, France, 30 May – 1 June, (2016).

8 Hesthaven, J. S. and Warburton, T. *Nodal Discontinuous Galerkin Methods Algorithms, Analysis, and Applications*, Springer, NY (2008).

9 Srivinas, S., Rao. A. K. and Rao. C. V. An Exact Analysis for Vibration of Simply Supported Homogenous and Laminated Thick Rectangular Plates, *Journal of Sound and Vibration*, **12** (2), 187-199, (1970).

10 LeVeque, R. J. *Finite-Volume Methods for Hyperbolic Problems*, Cambridge University Press, Cambridge, (2004).

11 Gardonio, P. and Elliott, S. J. ISVR Technical Report 227, Driving Point and Transfer Mobility Matrices for Thin Plates Excited in Flexure, (1998).

12 Wang, C. M. Natural Frequencies Formula for Simply Supported Mindlin Plates, *Journal of Vibration and Acoustics*, **116** (4), 536-540, (1994).